Article

J. Biol. Regul. Homeost. Agents. 2024; 38(5): 4075–4087
https://doi.org/10.23812/j.biol.regul.homeost.agents.20243805.323

Endothelial Progenitor Cell-Derived Exosomes Promote the Osteogenic Differentiation of Periosteum-Derived Stem Cells by Regulating METTL3 and SGK1

Yaozhang Zhang[1], Hong Zhang[2], Shaoxiong Zhang[3], Ruiying Zhong[1], Bohan Xiong[1], Xiaojun Lu[1], Dengjun Yang[1], Qiai Zhang[1], Fuke Wang[1,*]

[1]Department of Sports Medicine, The First Affiliated Hospital of Kunming Medical University, 650000 Kunming, Yunnan, China
[2]Department of Psychiatry, The First Affiliated Hospital of Kunming Medical University, 650000 Kunming, Yunnan, China
[3]Department of Orthopedics, The Sixth Affiliated Hospital of Kunming Medical University, 653100 Yuxi, Yunnan, China
*Correspondence: wfk.04@126.com (Fuke Wang)
Published: 1 May 2024

Background: Endothelial progenitor cells (EPCs) migrate to ischemic or injured sites to participate in angiogenesis, whereas periosteum-derived stem cells (PDSCs) can differentiate in multiple directions. This study aimed to investigate the roles and mechanisms of EPCs in promoting the osteogenic differentiation of PDSCs.

Methods: Alizarin red and alkaline phosphatase staining was conducted after 3, 7, and 14 days of co-culture to evaluate the osteogenic differentiation of PDSCs. Subsequently, exosomes were isolated from EPCs. Following 7 and 14 days of treatment with PDSCs, scanning electron microscope and alizarin red staining were performed. EPCs with methyltransferase-like 3 (METTL3) knockdown and PDSCs overexpressing serum and glucocorticoid-induced kinase 1 (SGK1) were constructed to further explore the underlying mechanism.

Results: As the co-culture time increased, the alkaline phosphatase and calcification levels gradually increased in the co-cultured group. EPC-derived exosomes also elevated alkaline phosphatase and calcification levels of PDSCs, and significantly upregulated osteopontin (OPN), osteoprotegerin (OPG), and runt-related transcription factor 2 (RUNX2) expression ($p < 0.05$). Both immunofluorescent staining and western blot revealed that treatment with the EPC-derived exosomes significantly enhanced the expression levels of METTL3 and SGK1 were significantly enhanced in PDSCs compared with those in control cells ($p < 0.05$). Exosomes were successfully isolated from EPCs with METTL3 knockdown; these exosomes significantly downregulated the expression levels of OPN, OPG, and RUNX2 ($p < 0.05$). SGK1 expression was significantly upregulated by EPC-derived exosomes in PDSCs overexpressing METTL3 ($p < 0.05$) and markedly downregulated in PDSCs treated with EPC-derived exosomes with METTL3 knockdown ($p < 0.05$).

Conclusions: EPC-derived exosomes carrying METTL3 may promote the osteogenic differentiation of PDSCs by regulating SGK1.

Keywords: EPC-derived exosomes; osteogenic differentiation; periosteum-derived stem cells; METTL3; SGK1

Introduction

The improved performance of tissue engineering presents an effective strategy for clinically repairing bone defects. Bone tissue is highly vascularized, and the interplay between vascularization and osteogenesis is integral. Enhancing angiogenesis can facilitate osteogenesis [1]. However, the rapidity of vascularization has always been a limiting factor in bone tissue engineering's osteogenic effect. The primary strategy involves the co-culture of osteoblasts with endothelial progenitor cells (EPCs) [2]. During osteogenesis, EPCs can migrate to ischemic or injured sites to engage in angiogenesis. When bone marrow mesenchymal stem cells (BMSCs) were co-cultured with EPCs to repair bone defects, EPCs were found to enhance BMSCs regenerative capabilities in rabbit radial bone defects [3]. Our previous study revealed that co-cultivating vascular endothelial cells and adipose-derived stem cells can promote the proliferation and osteogenic differentiation of adipose-derived stem cells [4]. Periosteum-derived stem cells (PDSCs), adult stem cells residing in the inner layer of the periosteum, exhibit surface markers of mesenchymal stem cells and possess the capacity to differentiate in multiple directions [5–7]. Furthermore, PDSCs share similar biological characteristics and differentiation potential with BMSCs, but excel in osteogenic differentiation, display better adaptability in the recipient environment after implantation, and sustain good osteogenic activity [8]. Consequently, this study aimed to elucidate the mechanisms through which EPCs influence in *in vitro* osteogenic differentiation of PDSCs.

Journal of
BIOLOGICAL REGULATORS
and Homeostatic Agents

The biological effects of EPCs are closely tied to exosomes. Exosomes are small membrane vesicles secreted by cells containing complex ribonucleic acids (RNAs) and proteins, usually between 40 and 200 nm in size [9]. Recent studies have unveiled that EPC-derived exosomes can safeguard blood vessels, promote the proliferation and migration of vascular endothelial cells, and exhibit anti-inflammatory, antioxidant, and anti-apoptotic effects on vascular endothelial cells. These properties make them pivotal in wound healing [10,11]. Another study proposed that osteoblast-derived exosomal circular RNA (circRNA) circ_0008542 might boost osteoclast-induced bone resorption through methyltransferase-like 3 (METTL3)-mediated N6-methyladenosine (m6A) methylation and competitive binding of microRNA (miR)-185-5p [12]. However, no studies have delved into the regulation of PDSCs by EPC-derived exosomes through m6A modification in tissue engineering bone. The m6A modification is the most significant and abundant form of RNA modification in eukaryotic cells [13], with a reversible process dynamically regulated by methyltransferase, binding protein, and demethylase [14]. Recent investigations have underscored m6A modification's pivotal role in bone formation and metabolism, with METTL3-mediated m6A modification participating in key processes such as cell differentiation and angiogenesis, during osteogenesis [15–17]. Tian *et al*. [18] demonstrated that METTL3 exhibited upregulation in osteogenic BMSCs and could expedite the osteogenic differentiation of BMSCs through the phosphorylated phosphatidylinositol 3 kinase (PI3K)-protein kinase B (AKT) signaling pathway. However, the effects and mechanisms of METTL3 in the EPC-derived exosomes on the osteogenic differentiation of PDSCs remain uncharted.

Serum and glucocorticoid-induced kinase 1 (SGK1), a serine/threonine protein kinase belonging to the protein kinases A, B and C (AGC) family, mediates downstream target protein phosphorylation through activation of the PI3K pathway. This activation regulates cell activities, including clinical physiological and pathological processes such as ion transport and vascular calcification [19]. Voelkl *et al*. [20] demonstrated that SGK1 could promote the osteogenic differentiation and calcification of vascular smooth muscle cells under hyperglycemic conditions. Additionally, Pietro *et al*. [21] reported that SGK1 can inhibit adipocyte differentiation by phosphorylating forkhead box O1 (FoxO1), which is closely related to the osteogenic differentiation of stem cells. These studies suggest that SGK1 represents a novel target for enhancing cell osteogenic differentiation and calcification. Therefore, this study aimed to investigate the mechanisms whereby EPCs promote the PDSC osteogenesis, with a focus on the roles of EPC-derived exosomes and m6A methylation regulation in promoting PDSC osteogenic differentiation.

Materials and Methods

Cell Culture and Identification

Human EPCs (Batch no. CP-R128) and PDSCs (Batch no. CP-R161) were purchased from Procell Life Science & Technology Co., Ltd., Wuhan, China. Based on the verification test, the cells did not contain mycoplasma, and based on Short Tandem Repeat (STR) results, the cell lines were indeed the EPC and PDSC lines. The EPCs were cultured in a special endothelial cell culture medium (Batch no. 1001, ScienCell Research Laboratories, San Diego, CA, USA), while PDSCs were cultured in Dulbecco's modified eagle medium (DMEM, Batch no. 11965092, Thermo Fisher Scientific, Waltham, MA, USA) with 10% fetal bovine serum (FBS, Batch no. 10099141C, Thermo Fisher Scientific, Waltham, MA, USA) and 1% penicillin-streptomycin (Batch no. 15140122, Thermo Fisher Scientific, Waltham, MA, USA). Both cells were maintained in an incubator with 5% CO_2 at 37 °C.

The expression levels of surface markers of EPCs (Recombinant Cluster Of Differentiation 34 (CD34), and CD133) and PDSCs (CD90, and CD105) were determined using an immunofluorescence assay. The cells were fixed with 4% paraformaldehyde (Batch no. 30525-89-4, SINOPHARM, Shanghai, China) for 30 min, dried for 10 min, and then incubated with 3% serum albumin for 20 min. Thereafter, the cells were incubated with the primary antibodies (anti-CD34, Batch no. ab81289; anti-CD133, Batch no. ab222782; anti-CD90, Batch no. ab307736; and anti-CD105, Batch no. ab252345; 1:1000; Abcam, Cambridge, UK) overnight at 4 °C, and then with the Cyanine (Cy3) fluorescein-labeled secondary antibody (Batch no. ab6939, 1:2000, Abcam, Cambridge, UK). After incubation at 37 °C for 30 min, the cells were washed three times with phosphate buffered saline (PBS), treated with 4′, 6-diaminidine-2 phenylindole (DAPI, Batch no. D1306, Thermo Fisher Scientific, Waltham, MA, USA) for 60 s, and sealed with 50% buffered glycerin. Finally, the cells were observed under a fluorescence microscope (MF52-N, Guangzhou Ming-Mei Photoelectric Technology Co. Ltd., Guangzhou, China).

Experimental Grouping

In the co-culture experiment with PDSCs and EPCs, the cells were divided into three groups: PDSCs, EPCs, and PDSCs + EPCs groups. In the PDSC and EPC groups, the PDSCs and EPCs were seeded at 1×10^5 cells/well in 6-well plates, respectively. In the PDSC + EPC group, PDSCs were seeded at 1×10^5 cells/well in a 6-well plate, while EPCs were seeded at 1×10^5 cells/well in a Transwell. The Transwell was then placed in a 6-well plate to establish a non-contact co-culture model. All cells in the different groups were cultured at 37 ℃ in a 5% CO_2 incubator. All observations under a microscope were recorded after 2 weeks of co-culture. During the culture process,

cells in the PDSC group were cultured in an osteogenic induction medium, while those in the PDSCs + EPCs group were maintained in a mixed medium (endothelial cell culture medium: osteogenic induction medium = 1:1).

In the experiment exploring the effect of EPC-derived exosomes on the osteogenic differentiation of PDSCs, the cells were divided into four groups: negative control (NC), PDSCs + EPCs-Exo (EPCs-Exo), PDSCs + sh-METTL3-EPCs-Exo (sh-METTL3-EPCs-Exo), and OE-METTL3-PDSCs groups.

Alizarin Red and Alkaline Phosphatase Staining

For alizarin red staining, after 3, 7, and 14 days of culture, cells in the different groups were fixed with 4% paraformaldehyde at room temperature for 30 min, washed three times with PBS, and treated with 0.5% alizarin red (Batch no. G8550, Solarbio, Beijing, China). After staining for 10 min in a shaker, the excess dye was removed, and the cells were washed with PBS. An inverted microscope was used to observe the bone calcium secretion of cells in the different groups.

For alkaline phosphatase staining, after 3, 7, and 14 days of culture, the cells were fixed with 4% paraformaldehyde at room temperature for 30 min and then stained in the dark using an alkaline phosphatase color developing kit (Batch no. P0321S, Beyotime, Shanghai, China), according to the manufacturer's instructions. After the reaction was stopped, the alkaline phosphatase staining area of cells in each group was observed under a microscope. If the alkaline phosphatase staining was positive, the cytoplasm was blue-purple and comprised blue-purple particles.

Extraction and Characterization of Exosomes from EPCs

The supernatant of EPCs was collected and centrifuged at 300 ×g for 10 min at 4 °C, followed by 2000 ×g for 10 min at 4 °C, 10,000 ×g for 30 min at 4 °C, and 100,000 ×g for 70 min at 4 °C. The sediment was resuspended with PBS, and the exosomes were obtained via centrifugation at 100,000 ×g for 70 min at 4 °C.

The concentration of the isolated exosomes was measured using a bicinchoninic acid (BCA) assay kit (Batch no. P0012S, Beyotime, Shanghai, China). Subsequently, the morphology and ultrastructure of the isolated exosomes were observed using transmission electron microscopy (TEM; Batch no. JEM-1230, JEOL LTD, Showima, Tokyo, Japan), as described in a previous study [22]. A Nanosight particle size analyzer (NTA; Batch no. NS300, Malvern Panaco Ltd., Malvern, UK) was employed to measure the size and particle distribution of exosomes, according to the manufacturer's protocols. Furthermore, the expression of the exosome-specific markers, including CD9 (Batch no. ab236630, Abcam, Cambridge, UK), CD63 (Batch no. ab134045, Abcam, Cambridge, UK), and CD81 (Batch no. ab79559, Abcam, Cambridge, UK), and the negative control (Calnexin, Batch no. ab22595, Abcam, Cambridge, UK), was detected via western blot analysis with the corresponding antibodies (1:1000) based on the method of Gao *et al*. [23].

The PDSCs at the logarithmic growth stage were seeded at 1×10^5 cells/well in a 6-well plate and treated with 5×10^7 particles/well of EPC-derived exosomes. After 24 h of co-culture, the treated cells were harvested and cultured in the osteogenic induction medium for further experiments.

Scanning Electron Microscope Analysis

The cells subjected to different treatments were washed and placed in a penicillin vial. Thereafter, the cells were fixed with 3% pre-cooled glutaraldehyde at 4 °C for 2 h. After the removal of the fixator and two rinses with PBS for 10 min each, 1% pre-cooled osmic acid was added to fix the cells at 4 °C for 1 h. After washing with PBS, the cells were dehydrated with 30%–100% gradient alcohol, and each concentration of alcohol was applied twice for 15 min each. The morphology and structure of the cells in each group were observed by freeze-drying and spraying platinum-palladium alloy under a scanning electron microscope (SEM, Batch no. HT7800, HITACHI, Chiyoda Ward, Tokyo, Japan).

Immunofluorescence (IF) Staining

The cells after osteogenic induction and differentiation for 14 days were harvested and washed three times with pre-heated PBS. Thereafter, the cells were fixed with 4% paraformaldehyde at room temperature for 20 min and washed three times with PBS. The cells were permeabilized with 0.1% Triton for 30 min and sealed with 3% bovine serum albumin (BSA, Batch no. S9010, Solarbio, Beijing, China) overnight at 27 °C. On day 2, the cells were incubated with the primary antibody (anti-SGK1, Batch no. ab43606, 1:1000, Abcam, Cambridge, UK) overnight at 4 °C, followed by the fluorescent-labeled secondary antibody at 37 °C for 1 h. Finally, the cells were stained with DAPI for 10 min and observed using a fluorescence microscope to obtain photographic records.

Acquisition of Lentivirus Packaging and Cell Transfection

The OE-METTL3 vector and sh-METTL3 vector were constructed and provided by Shanghai GenePharma Co., Ltd. (Shanghai, China). The sequences of METTL3 shRNA were shown as follow: sh-METTL3-1, sense, 5′-GCCTTAACATTGCCCACTGAT-3′, anti-sense, 5′-ATCAGTGGGCAATGTTAAGGC-3′; sh-METTL3-2, sense, 5′-GCAAGTATGTTCACTATGAAA-3′, anti-sense, 5′-TTTCATAGTGAACATACTTGC-3′; as well as the sequence of negative control (NC) was sense, 5′-AATTCTCCGAACGTGTCACGT-3′, and anti-sense, 5′-ACGTGACACGTTCGGAGAATT-3′. The methods of

Journal of
BIOLOGICAL REGULATORS
and Homeostatic Agents

lentivirus packaging of the OE-METTL3 and sh-METTL3 vectors were described previously [24]. To construct the PDSCs with METTL3 overexpression, the PDSCs (3×10^5/well) were seeded in a 6-well plate, and DMEM with 10% FBS was added to each well. After overnight culture, the OE-METTL3 vector (multiplicity of infection [MOI] = 30) was added to the cells, and after 12 h of culture, the medium was changed. After continued culture for 3 days, the expression of METTL3 with green fluorescence was observed under an inverted fluorescence microscope. Purinomycin (Batch no. A1113803, 1 mg/mL, Thermo Fisher Scientific, Waltham, MA, USA) was subsequently added to screen the transfected cells, and after 7 days of screening, the stable cell lines (OE-METTL3-PDSCs) were obtained.

To establish the EPCs with METTL3 knockdown, 2 μg of the sh-METTL3-1/2 vector was transfected into EPCs using Lipofectamine 2000 (Batch no. 11668019, Thermo Fisher Scientific, Waltham, MA, USA) in accordance with the manufacturer's recommendations. After 48 h of transfection, purinomycin (1 mg/mL) was added to screen the transfected cells, and after 7 days of screening, the stable cell lines (sh-METTL3-EPCs) were obtained and used for the subsequent study.

Western Blot

Total protein was isolated from cells subjected to different treatments using Radio Immunoprecipitation Assay (RIAP) lysis buffer (Batch no. abs9228, Aibixin (Shanghai) Biotechnology Co., Ltd., Shanghai, China) and quantified using a BCA assay kit. Thereafter, 20 μg of the protein sample was separated via 10% sodium dodecyl sulfate-polyacrylamide gel electrophoresis (SDS-PAGE), transferred onto polyvinylidene fluoride (PVDF) membranes, and blocked with 3% BSA at room temperature for 1 h. After washing, the membranes were incubated with primary antibodies against osteopontin (OPN, Batch no. ab75285, 1:1000, Abcam, Cambridge, UK), osteoprotegerin (OPG, Batch no. ab183910, 1:1000, Abcam, Cambridge, UK), runt-related transcription factor 2 (RUNX2, Batch no. ab23981, 1:1000, Abcam, Cambridge, UK), METTL3 (Batch no. ab240595, 1:1000, Abcam, Cambridge, UK), SGK1 (Batch no. ab43606, 1:1000, Abcam, Cambridge, UK), and glyceraldehyde 3-phosphate dehydrogenase (GAPDH, Batch no. ab9485, 1:1000, Abcam, Cambridge, UK) overnight at 4 °C, followed by the corresponding secondary antibodies (Batch no. 111-035-003, and 115-035-003, 1:5000, Jackson ImmunoResearch, West Grove, PA, USA) at room temperature for 1 h. The protein bands were developed using an enhanced chemiluminescence luminescent solution and exposed to the chemiluminescence imager (Batch no. 36208ES60, Tanon 4100, Tanon Science & Technology, Shanghai, China). ImageJ software (version 1.8.0, National Institutes of Health, Bethesda, MD, USA) was employed to analyze the grayscale values of each band, and GAPDH was used as the internal reference. The relative expression of each protein was calculated using the grayscale of the target band or the grayscale of the internal reference band.

Statistical Analysis

Data are expressed as mean ± standard deviation (SD), and GraphPad prism 5 (version 5.0, GraphPad Software, San Diego, CA, USA) was used for the statistical analyses. A student's *t*-test was used to compare two groups, and one-way analysis of variance (ANOVA) followed by Tukey's test was employed to compare more than two groups. $p < 0.05$ was considered to indicate statistical significance.

Results

Identification of Cell Morphology

Based on microscopy, PDSCs exhibited an ellipsoid shape (Fig. 1A), while EPCs were spindle-shaped with regular cell morphology (Fig. 1B). The surface markers of PDSCs and EPCs were detected using immunofluorescence staining. CD90 and CD105 were found to be expressed in PDSCs (Fig. 1C), while CD34 and CD133 were expressed in EPCs (Fig. 1D). These results indicate that the two stem cells represented PDSCs and EPCs and could be used for the subsequent experiments.

Characterization of the EPC-Derived Exosomes

EPCs were used for exosome extraction, and TEM, NTA, and western blot were conducted to characterize the extracted exosomes. TEM revealed that the morphology of the extracted substances was nearly round or cup-shaped, with a diameter of approximately 100 nm (Fig. 2A). The NTA results revealed that our extracted exosomes were 50–200 nm in diameter and approximately 500 nm^3 in volume (Fig. 2B). Based on western blot analysis, the exosome-specific markers CD9, CD63, and CD81, were expressed in the extracted exosomes, whereas the negative control, Calnexin, was not expressed in the exosomes (Fig. 2C). The results indicate that the exosomes were successfully isolated from EPCs.

EPCs Promote the Osteogenic Differentiation of PDSCs after Co-Culture

After EPCs and PDSCs were co-cultured for 3, 7, and 14 days, the level of alkaline phosphatase was found to be higher than that in the culture of individual cells ($p < 0.05$); this level gradually elevated as the culture time proceeded (Fig. 3A). Based on Alizarin red staining, compared with individual cell culture, the calcification level and staining degree of PDSCs were significantly increased in the co-culture group and enhanced as the culture time proceeded ($p < 0.05$, Fig. 3B). These results indicate that EPCs could promote the osteogenic differentiation of PDSCs after co-culture.

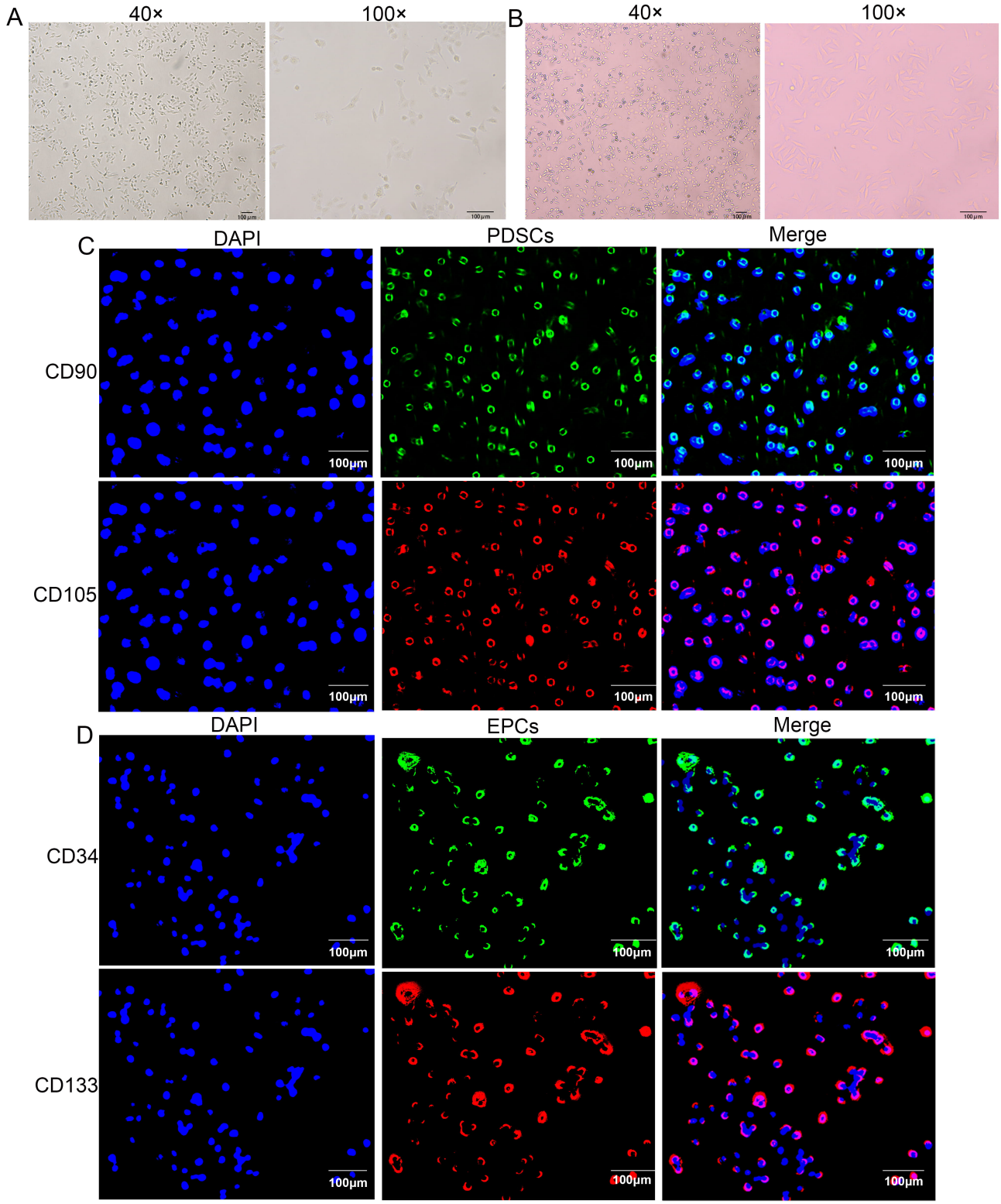

Fig. 1. Identification of periosteum-derived stem cells (PDSCs) and endothelial progenitor cells (EPCs). (A) Morphology of PDSCs based on microscopy at magnifications of 40× and 100×. Scale bar = 100 μm. N = 3. (B) Morphology of EPCs based on microscopy at magnifications of 40× and 100×. Scale bar = 100 μm. N = 3. (C) Expression of PDSC-surface markers (CD90, and CD105) based on the immunofluorescence assay. Scale bar = 100 μm. N = 3. (D) Expression of EPC-surface markers (CD34, and CD133) based on the immunofluorescence assay. Scale bar = 100 μm. N = 3. DAPI, 4′, 6-diaminidine-2 phenylindole; CD, Recombinant Cluster Of Differentiation.

Journal of
BIOLOGICAL REGULATORS
and Homeostatic Agents

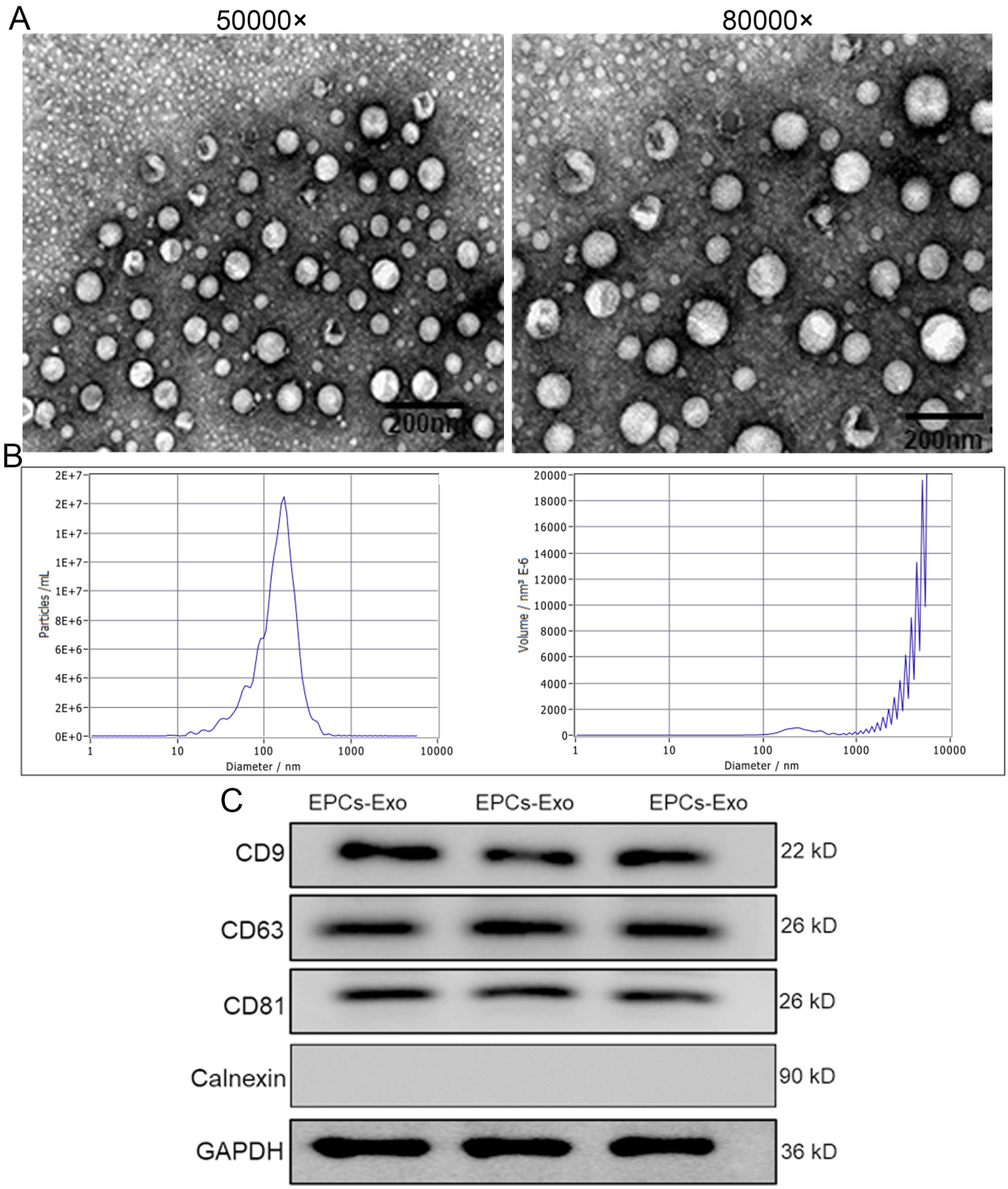

Fig. 2. Characterization of the endothelial progenitor cells (EPCs)-derived exosomes. (A) Morphology of the isolated exosomes based on transmission electron microscopy. Scale bar = 200 nm. (B) The particle size of the isolated exosomes based on a Nanosight particle size analyzer. (C) Expression of exosome-specific markers based on western blot analysis. EPCs-Exo, EPC-derived exosomes. N = 3. GAPDH, glyceraldehyde 3-phosphate dehydrogenase.

EPC-Derived Exosomes Promote the Osteogenic Differentiation of PDSCs

To explore the mechanisms whereby EPCs promote the osteogenic differentiation of PDSCs, researchers isolated exosomes from EPCs and added to PDSCs. After 7 and 14 days of treatment, the PDSCs treated with EPC-derived exosomes had better osteogenic effects than the PDSCs without treatment (Fig. 4A). Alizarin red staining revealed that the calcification level and staining degree of PDSCs were increased after EPC-derived exosome

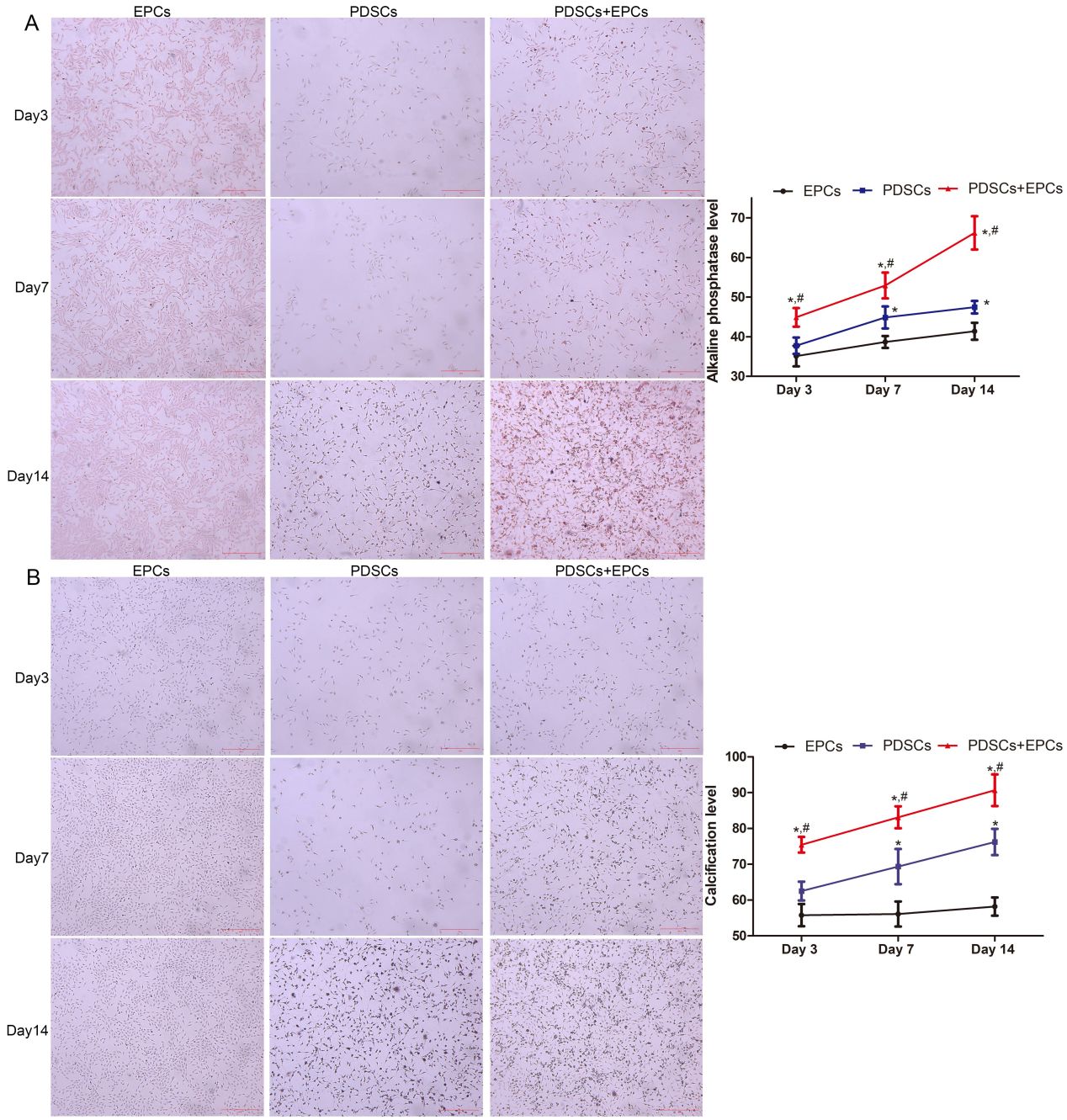

Fig. 3. EPCs promote the osteogenic differentiation of PDSCs via co-culture. (A) Alkaline phosphatase level in the PDSCs after co-culture with EPCs based on an alkaline phosphatase color developing kit. Scale bar = 50 μm. N = 3. (B) Calcification level of PDSCs after co-culture with EPCs based on alizarin red staining. Scale bar = 50 μm. N = 3. *: $p < 0.05$, compared with the EPCs; $^{\#}$: $p < 0.05$, compared with the PDSCs.

treatment relative to those of untreated PDSCs ($p < 0.05$, Fig. 4B). Furthermore, the markers of osteogenic differentiation (OPN, OPG, and RUNX2) were detected using western blot analysis. Compared with the control group, the expression levels of OPN, OPG, and RUNX2 were significantly upregulated in PDSCs treated with EPC-derived exosomes ($p < 0.05$, Fig. 4C). These results imply that EPCs could promote the osteogenic differentiation of PDSCs via paracrine exosomes.

Effects of METTL3/SGK1 on the Osteogenic Differentiation of PDSCs

Compared with the control group, both immunofluorescent staining and western blot revealed that, compared with the control group, the expression levels of METTL3 and SGK1 were significantly enhanced in the group treated with the EPC-derived exosomes ($p < 0.05$, Fig. 5A,B).

To verify the roles of EPC-derived exosomal METTL3/SGK1 in the osteogenic differentiation of

Journal of
BIOLOGICAL REGULATORS
and Homeostatic Agents

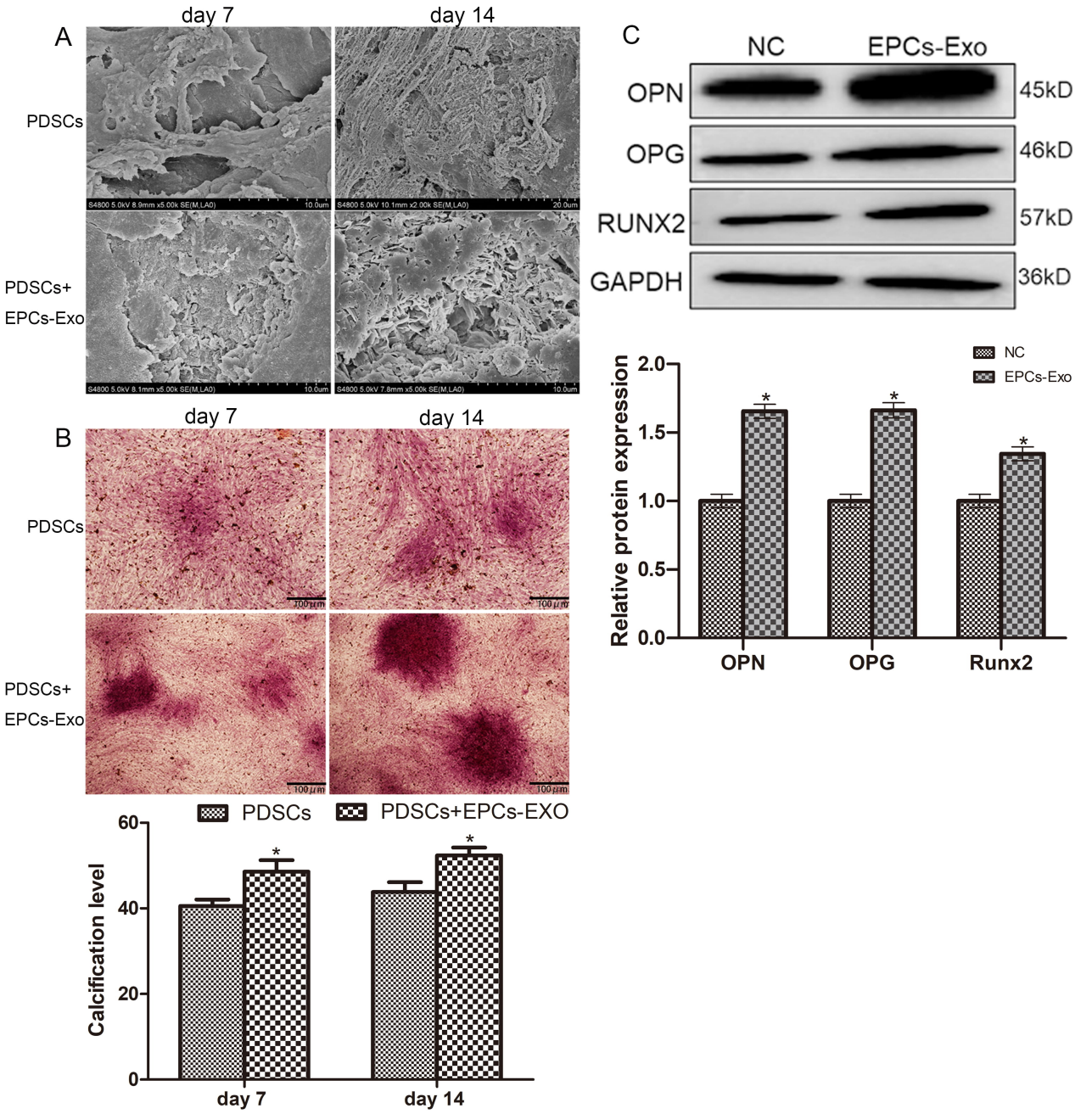

Fig. 4. EPC-derived exosomes promote the osteogenic differentiation of PDSCs. (A) Morphology and structure of cells treated with EPC-derived exosomes for 7 and 14 days based on scanning electron microscopy. N = 3. (B) Calcification level of PDSCs after co-culture with the EPC-derived exosomes based on alizarin red staining. Scale bar = 100 μm. N = 3. *: $p < 0.05$, compared with the PDSCs. (C) Expression of osteogenic differentiation-related markers (osteopontin (OPN), osteoprotegerin (OPG), and runt-related transcription factor 2 (RUNX2)) in PDSCs based on western blot. *: $p < 0.05$, compared with the NC group. N = 3. NC: PDSCs cultured in osteogenic induction medium; EPCs-EXO: PDSCs treated with EPCs-EXO for 24 h and then cultured in osteogenic induction medium.

PDSCs, EPCs with METTL3 knockdown were established. Western blot analysis revealed no significant difference in METTL3 expression between the blank control and negative controls ($p > 0.05$, Fig. 6A). Compared with the blank control group, the expression of METTL3 was significantly downregulated in the cell group transfected with sh-METTL3-1 and sh-METTL3-2 ($p < 0.05$). Further, the effect of sh-METTL3-2 was better than that of sh-METTL3-1 (Fig. 6A). Therefore, based on further experiments, exosomes were isolated from the EPCs with METTL3 knockdown. PDSCs were treated with EPC-derived exosomes and EPCs with METTL3 knockdown-derived exosomes. Thereafter, the markers of osteogenic differentiation (OPN, OPG, and RUNX2) were

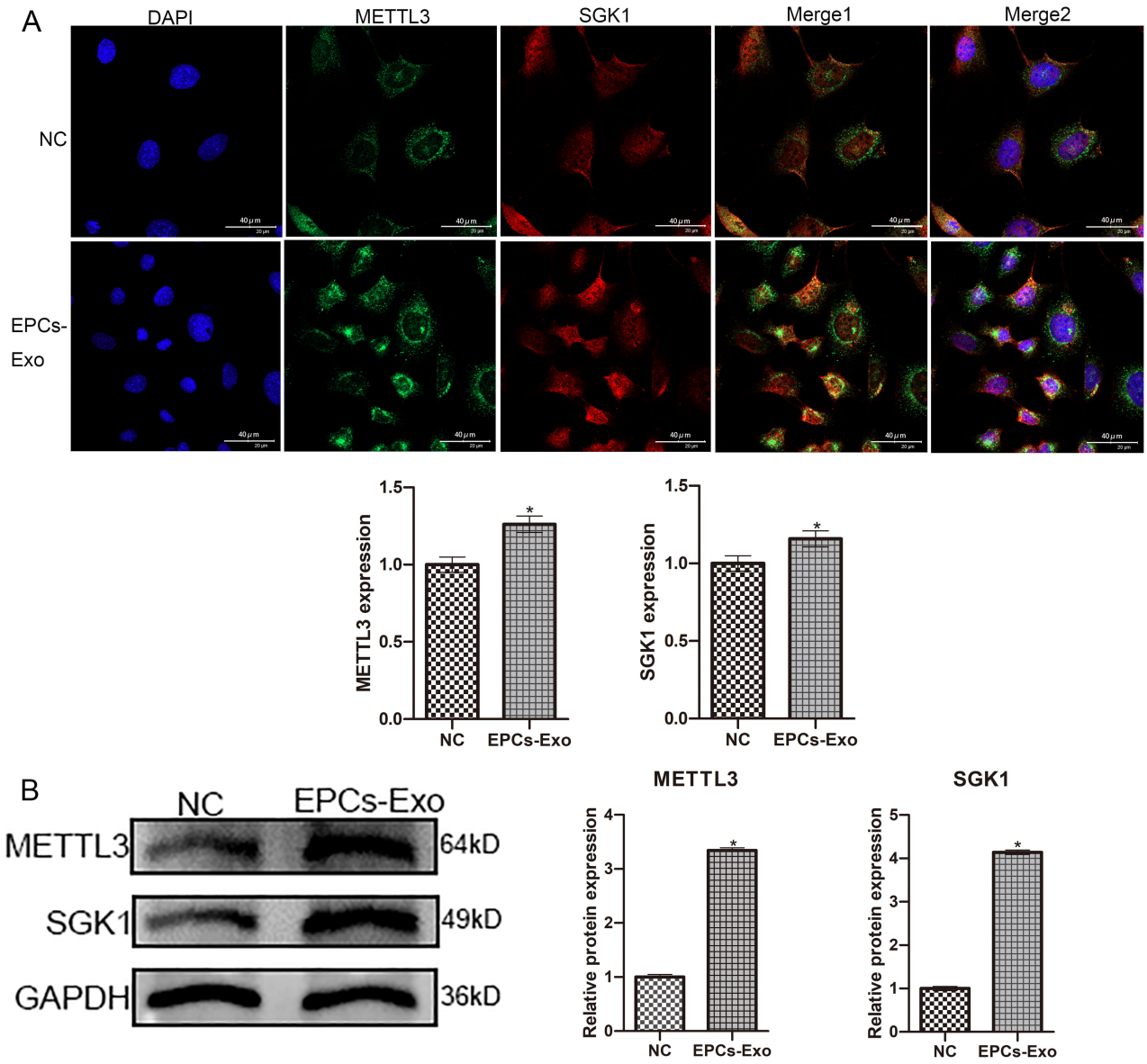

Fig. 5. Expression of methyltransferase-like 3 (METTL3) and serum and glucocorticoid-induced kinase 1 (SGK1) in PDSCs after treatment with the EPC-derived exosomes. (A) Expression of METTL3 and SGK1 in PDSCs after treatment with EPC-derived exosomes using immunofluorescent staining. Scale bar = 40 μm. N = 3. (B) Protein expression of METTL3 and SGK1 in PDSCs after treatment with EPC-derived exosomes based on western blot. *: $p < 0.05$, compared with the NC group. N = 3. NC: PDSCs cultured in osteogenic induction medium; EPCs-EXO: PDSCs treated with EPCs-EXO for 24 h and then cultured in osteogenic induction medium.

determined using a western blot. Evidently, the expression levels of OPN, OPG, and RUNX2 were significantly increased in the group treated with the EPC-derived exosomes compared with the NC group ($p < 0.05$), and reduced in the group treated with EPCs with METTL3 knockdown-derived exosomes compared with the group treated with the EPC-derived exosomes ($p < 0.05$, Fig. 6B).

PDSCs with METLL3 overexpression were constructed to investigate the interaction between METTL3 and SGK1. Compared with the control group, SGK1 expression was significantly upregulated in the group treated with the EPC-derived exosomes ($p < 0.05$) and markedly downregulated in the group treated with EPCs with METTL3 knockdown-derived exosomes ($p < 0.05$, Fig. 6C). However, SGK1 expression in the PDSC group overexpressing METTL3 was significantly higher than that in the NC group ($p < 0.05$, Fig. 6C). The results indicate that EPC-derived exosomes may promote the osteogenic differentiation of PDSCs through METTL3/SGK1.

Discussion

Compared with BMSCs, PDSCs, as directed bone progenitor cells, have stronger osteogenic ability and better stability of directed differentiation [8,25]. According to a pre-

Journal of
BIOLOGICAL REGULATORS
and Homeostatic Agents

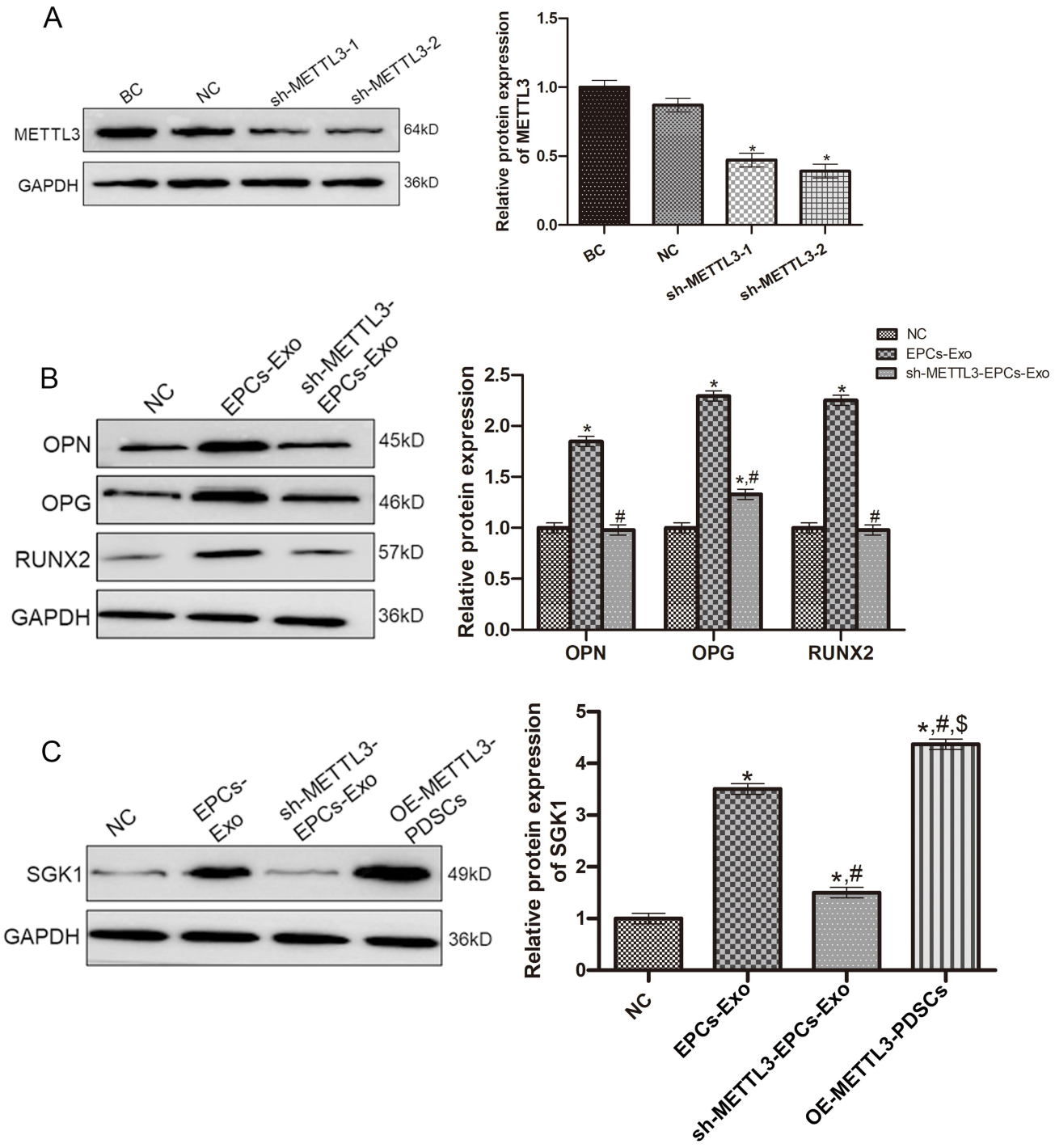

Fig. 6. Effects of METTL3/SGK1 on the osteogenic differentiation of PDSCs. (A) Expression of METTL3 in the EPCs transfected with sh-MELLT3. *: $p < 0.05$, compared with the BC group. N = 3. BC, blank control (control EPCs); NC, negative control (EPCs transfected with sh-NC); sh-METTL3-1/sh-METTL3-2, EPCs transfected with sh-METTL1/sh-METTL2. (B) Protein expression of OPN, OPG, and RUNX2 in the PDSCs treated with EPC-derived exosomes and EPCs with METTL3 knockdown-derived exosomes. *: $p < 0.05$, compared with the NC group; #: $p < 0.05$, compared with the EPCs-Exo group. N = 3. (C) Protein expression of SGK1 in PDSCs treated with EPC-derived exosomes, EPCs with METTL3 knockdown-derived exosomes, and PDSCs overexpressing METTL3. *: $p < 0.05$, compared with the NC group; #: $p < 0.05$, compared with the EPC-Exo group; $: $p < 0.05$, compared with the sh-METTL3-EPCs-Exo group. N = 3. NC, PDSCs cultured in osteogenic induction medium; EPCs-EXO, PDSCs treated with EPCs-EXO for 24 h and then cultured in osteogenic induction medium; sh-METTL3-EPCs-EXO, PDSCs treated with EPCs with METTL3 knockdown-derived exosomes; OE-METTL3-PDSCs, PDSCs with METTL3 overexpression.

vious study, when mouse PDSCs were co-transplanted with collagen calcium phosphate scaffolds and endothelial cells *in vivo*, the angiogenesis potential was increased, which revealed pericyte cells that induce hematopoietic matrix and new angiogenesis [26]. Zheng *et al*. [27] illustrated that loading PDSCs onto a polylactic-glycolic acid scaffold containing allogenic serum could increase the expression of osteocalcin, osteonectin, and type 1 collagen in 3D culture, thereby promoting osteogenesis. In our study, PDSCs were verified to have strong proliferation and stable directional differentiation ability under *in vitro* culture and could express MSC-related markers (CD90 and CD105), which further indicated the excellent osteogenic effects of PDSCs.

At present, achieving vascularization in the field of bone tissue engineering is still reliant on the co-cultivation of osteoblasts and EPCs [2], which has been proven in many recent studies [28,29]. EPCs have been demonstrated to have great potential in the vascularization of tissue engineering bones. For example, Kong *et al*. [30] demonstrated that EPCs could improve angiogenesis activity in the fracture area of rats through the hypoxia-inducible factor-1α (HIF-1α)/ endothelial nitric oxide synthase (eNOS)/ nitric oxide (NO) axis, and promote fracture healing. Xu *et al*. [31] revealed that EPCs significantly promoted the vascularization of BMSCs, and co-transplantation of EPCs and BMSCs was used to treat steroid-induced femoral head necrosis. In addition to accelerating vascularization, co-culture of EPCs with target cells significantly promotes bone formation. Zhao *et al*. [3] revealed that the co-culture of EPCs and BMSCs could not only accelerate the repair of bone defects but also promote the formation of blood vessels and bone on the scaffold. Our study revealed that EPCs and EPC-derived exosomes promoted the osteogenic differentiation of PDSCs. Therefore, in the field of bone tissue engineering, co-culture of PDSCs with EPCs may be a crucial strategy for promoting vascularization and osteogenesis.

Although current studies have confirmed the promoting effects of co-culture with EPCs on the osteogenesis of PDSCs, the mechanisms by which it promotes osteogenesis are not yet clear. Recently, EPC-derived exosomes have been reported to have various activities and functions and play significant roles in damage repair and tissue regeneration [32,33]. Exosomes, as the primary mode of the paracrine pathway interaction between cells, contain abundant proteins, RNA, and deoxyribonucleic acid (DNA, etc., which may be the main carriers for the functioning of EPCs [34]. Zha *et al*. [35] reported that chondrogenic progenitor ATDC5-derived exosomes carrying vascular endothelial growth factor (VEGF) plasmids could promote osteogenic induction and vascular remodeling in large segmental bone defects. Another study revealed that CD34+ EPCs derived from human umbilical cord blood could stimulate the osteogenic differentiation of human periosteum-derived osteoblasts [36]. Similarly, our experiments confirmed that EPC-derived exosomes upregulated OPN, OPG, and RUNX expression and promoted the osteogenic differentiation of PDSCs, which implied that EPCs may regulate the osteogenic process of PDSCs by secreting exosomes.

Based on the complex components in the exosomes, current studies revealed that EPCs exert biological effects through various components in the exosomes, including miRNAs, long non-coding RNAs (lncRNAs), cytokines (VEGF, and fibroblast growth factor [FGF]), or target genes [37]. Cui *et al*. [38] found that the expression of the lncRNA, MALAT1, was higher in the EPC-derived exosomes and directly interacted with miR-124 to regulate integrin beta 1 (ITGB1) expression, thereby enhancing the recruitment and differentiation of osteoclast precursors and promoting bone repair *in vivo*. Another study revealed that during distraction osteogenesis, EPC-derived exosomes could accelerate bone regeneration by downregulating sprouty-related EVH1 domain-containing protein 1 (SPRED1) and activating Raf/extracellular regulated protein kinases (ERK) signaling to stimulate angiogenesis [39]. M6A has recently been reported to play a role in pluripotent differentiation and the development of cell lineages, including the osteogenic differentiation of BMSCs [40]. METTL3, a member of m6A writers, is observed to have pivotal functions in the differentiation of BMSCs and adipogenesis [41]. Wu *et al*. [42] clarified that METTL3 silencing could lead to impaired bone formation, insufficient osteogenic differentiation potential, and increased bone marrow obesity, while its overexpression could protect mice from estrogen deficiency-induced osteoporosis. Zhang *et al*. [43] demonstrated that the expression of the m6A methyltransferase, METTL3, increased during osteoblast differentiation, whereas METTL3 deficiency could suppress osteoblast differentiation and mineralization. Based on our results, EPC-derived exosomes upregulated METTL3 and the osteogenic-related indicators in PDSCs, and the knockdown of METTL3 in the EPC-derived exosomes could inhibit the action of EPC-derived exosomes in the osteoblastic differentiation of PDSCs, which indicated that METTL3 is indeed a promoting factor for osteoblastic differentiation of PDSCs.

Using high-throughput RNA sequencing and bioinformatics analysis, Liu *et al*. [44] predicted that SGK1 might be involved in the potential molecular mechanism for the osteogenic differentiation of BMSCs, providing an underlying molecular target for studying bone defects. SGK1, a pivotal molecule in different signal transduction pathways and cell phosphorylation cascades, is abnormally expressed in cancer tissues and plays an important role in cell proliferation, differentiation, and ion channel regulation [45]. In our study, SGK1 was upregulated in PDSCs treated with EPC-derived exosomes but was downregulated in PDSCs induced by shMETTL3-EPC-derived exosomes. To eliminate the interference of exogenous factors, PDSCs overexpressing MTLLE3 were constructed, which resulted in in-

Journal of BIOLOGICAL REGULATORS and Homeostatic Agents

creased expression of SGK1. Taken together, we speculate that the upregulation of SGK1 expression in the osteoblast differentiation of PDSCs may be caused by METTL3.

Conclusions

The co-culture of EPCs and PDSCs can rapidly and efficiently induce osteogenic differentiation. In addition, exosomes secreted by EPCs carrying METTL3 may promote the osteogenic differentiation of PDSCs by regulating SGK1. Our findings imply that METTL3 and SGK1 might be new targets for the regulation of osteogenic differentiation and provide good theoretical support for the future clinical application of PDSC in the treatment of bone defects in bone tissue engineering.

Availability of Data and Materials

The dataset used and/or analysed during the current study are available from the corresponding author on a reasonable request.

Author Contributions

Conception and design of the research: YZZ and FKW; Acquisition of data: YZZ, HZ, QAZ, and RYZ; Formal analysis and investigation: SXZ, BHX, DJY, and XJL; Funding: FKW; Writing — original draft preparation: YZZ; Writing — review and editing: FKW, DJY, and QAZ; Supervision: FKW. All authors contributed to editorial changes in the manuscript. All authors read and approved the final manuscript. All authors have participated sufficiently in the work and agreed to be accountable for all aspects of the work.

Ethics Approval and Consent to Participate

Not applicable.

Acknowledgment

Not applicable.

Funding

This study was supported by Yunnan Provincial High Level Talent Training Support Program Famous Medical Project (RLMY2020009).

Conflict of Interest

The authors declare no conflict of interest.

References

[1] Diomede F, Marconi GD, Fonticoli L, Pizzicanella J, Merciaro I, Bramanti P, *et al*. Functional Relationship between Osteogenesis and Angiogenesis in Tissue Regeneration. International Journal of Molecular Sciences. 2020; 21: 3242.

[2] Simunovic F, Finkenzeller G. Vascularization Strategies in Bone Tissue Engineering. Cells. 2021; 10: 1749.

[3] Zhao X, Han XS, Zhou QZ, Liu BY, Yang B, Gong Z, *et al*. Repair of Bone Defects With Endothelial Progenitor Cells and Bone Marrow-Derived Mesenchymal Stem Cells With Tissue-Engineered Bone in Rabbits. Annals of Plastic Surgery. 2020; 85: 430–436.

[4] Wang FK, Zhang H, Li YL, Liu L, He C, Cai GF, *et al*. Vascular endothelial cells and adipose stem cells were cultured to construct ectopic osteogenesis of tissue engineered bone. Zhongguo Xiu Fu Chong Jian Wai Ke Za Zhi = Zhongguo Xiufu Chongjian Waike Zazhi = Chinese Journal of Restorative and Reconstructive Surgery. 2019; 33: 1310–1319. (In Chinese)

[5] Wang Q, Huang C, Zeng F, Xue M, Zhang X. Activation of the Hh pathway in periosteum-derived mesenchymal stem cells induces bone formation in vivo: implication for postnatal bone repair. The American Journal of Pathology. 2010; 177: 3100–3111.

[6] Jeyaraman M, Muthu S, Gangadaran P, Ranjan R, Jeyaraman N, Prajwal GS, *et al*. Osteogenic and Chondrogenic Potential of Periosteum-Derived Mesenchymal Stromal Cells: Do They Hold the Key to the Future? Pharmaceuticals (Basel, Switzerland). 2021; 14: 1133.

[7] Ferretti C, Mattioli-Belmonte M. Periosteum derived stem cells for regenerative medicine proposals: Boosting current knowledge. World Journal of Stem Cells. 2014; 6: 266–277.

[8] Duchamp de Lageneste O, Julien A, Abou-Khalil R, Frangi G, Carvalho C, Cagnard N, *et al*. Periosteum contains skeletal stem cells with high bone regenerative potential controlled by Periostin. Nature Communications. 2018; 9: 773.

[9] Krylova SV, Feng D. The Machinery of Exosomes: Biogenesis, Release, and Uptake. International Journal of Molecular Sciences. 2023; 24: 1337.

[10] Salybekov AA, Kunikeyev AD, Kobayashi S, Asahara T. Latest Advances in Endothelial Progenitor Cell-Derived Extracellular Vesicles Translation to the Clinic. Frontiers in Cardiovascular Medicine. 2021; 8: 734562.

[11] Pan MC, Lin XY, Wang H, Chen YF, Leng M. Research advances on the roles of exosomes derived from vascular endothelial progenitor cells in wound repair. Zhonghua Shao Shang Za Zhi = Zhonghua Shaoshang Zazhi = Chinese Journal of Burns. 2020; 36: 883–886. (In Chinese)

[12] Wang W, Qiao SC, Wu XB, Sun B, Yang JG, Li X, *et al*. Circ_0008542 in osteoblast exosomes promotes osteoclast-induced bone resorption through m6A methylation. Cell Death & Disease. 2021; 12: 628.

[13] Deng LJ, Deng WQ, Fan SR, Chen MF, Qi M, Lyu WY, *et al*. m6A modification: recent advances, anticancer targeted drug discovery and beyond. Molecular Cancer. 2022; 21: 52.

[14] Chen J, Fang Y, Xu Y, Sun H. Role of m6A modification in female infertility and reproductive system diseases. International Journal of Biological Sciences. 2022; 18: 3592–3604.

[15] Wang HF, Kuang MJ, Han SJ, Wang AB, Qiu J, Wang F, *et al*. BMP2 Modified by the m^6A Demethylation Enzyme ALKBH5 in the Ossification of the Ligamentum Flavum Through the AKT Signaling Pathway. Calcified Tissue International. 2020; 106: 486–493.

[16] Yuan X, Shi L, Guo Y, Sun J, Miao J, Shi J, *et al*. METTL3 Regulates Ossification of the Posterior Longitudinal Ligament via the lncRNA XIST/miR-302a-3p/USP8 Axis. Frontiers in Cell and Developmental Biology. 2021; 9: 629895.

[17] Li D, Cai L, Meng R, Feng Z, Xu Q. METTL3 Modulates Osteoclast Differentiation and Function by Controlling RNA Stability and Nuclear Export. International Journal of Molecular Sciences. 2020; 21: 1660.

[18] Tian C, Huang Y, Li Q, Feng Z, Xu Q. Mettl3 Regulates Osteogenic Differentiation and Alternative Splicing of Vegfa in Bone Marrow Mesenchymal Stem Cells. International Journal of Molecular Sciences. 2019; 20: 551.

[19] Lang F, Stournaras C, Zacharopoulou N, Voelkl J, Alesutan I. Serum- and glucocorticoid-inducible kinase 1 and the response to cell stress. Cell Stress. 2018; 3: 1–8.

[20] Voelkl J, Luong TT, Tuffaha R, Musculus K, Auer T, Lian X, *et al*. SGK1 induces vascular smooth muscle cell calcification through NF-κB signaling. The Journal of Clinical Investigation. 2018; 128: 3024–3040.

[21] Di Pietro N, Panel V, Hayes S, Bagattin A, Meruvu S, Pandolfi A, *et al*. Serum- and glucocorticoid-inducible kinase 1 (SGK1) regulates adipocyte differentiation via forkhead box O1. Molecular Endocrinology (Baltimore, Md.). 2010; 24: 370–380.

[22] Zhang Y, Wang X, Chen J, Qian D, Gao P, Qin T, *et al*. Exosomes derived from platelet-rich plasma administration in site mediate cartilage protection in subtalar osteoarthritis. Journal of Nanobiotechnology. 2022; 20: 56.

[23] Gao M, Yu T, Liu D, Shi Y, Yang P, Zhang J, *et al*. Sepsis plasma-derived exosomal miR-1-3p induces endothelial cell dysfunction by targeting SERP1. Clinical Science (London, England: 1979). 2021; 135: 347–365.

[24] Qiao H, Wang YF, Yuan WZ, Zhu BD, Jiang L, Guan QL. Silencing of ENO1 by shRNA Inhibits the Proliferation of Gastric Cancer Cells. Technology in Cancer Research & Treatment. 2018; 17: 1533033818784411.

[25] Radtke CL, Nino-Fong R, Esparza Gonzalez BP, Stryhn H, McDuffee LA. Characterization and osteogenic potential of equine muscle tissue- and periosteal tissue-derived mesenchymal stem cells in comparison with bone marrow- and adipose tissue-derived mesenchymal stem cells. American Journal of Veterinary Research. 2013; 74: 790–800.

[26] van Gastel N, Torrekens S, Roberts SJ, Moermans K, Schrooten J, Carmeliet P, *et al*. Engineering vascularized bone: osteogenic and proangiogenic potential of murine periosteal cells. Stem Cells (Dayton, Ohio). 2012; 30: 2460–2471.

[27] Zheng YX, Ringe J, Liang Z, Loch A, Chen L, Sittinger M. Osteogenic potential of human periosteum-derived progenitor cells in PLGA scaffold using allogeneic serum. Journal of Zhejiang University. Science. B. 2006; 7: 817–824.

[28] Esquiva G, Grayston A, Rosell A. Revascularization and endothelial progenitor cells in stroke. American Journal of Physiology. Cell Physiology. 2018; 315: C664–C674.

[29] Yu B, Chen Q, Le Bras A, Zhang L, Xu Q. Vascular Stem/Progenitor Cell Migration and Differentiation in Atherosclerosis. Antioxidants & Redox Signaling. 2018; 29: 219–235.

[30] Kong L, Wang Y, Wang H, Pan Q, Zuo R, Bai S, *et al*. Conditioned media from endothelial progenitor cells cultured in simulated microgravity promote angiogenesis and bone fracture healing. Stem Cell Research & Therapy. 2021; 12: 47.

[31] Xu H, Wang C, Liu C, Peng Z, Li J, Jin Y, *et al*. Cotransplantation of mesenchymal stem cells and endothelial progenitor cells for treating steroid-induced osteonecrosis of the femoral head. Stem Cells Translational Medicine. 2021; 10: 781–796.

[32] Zeng CY, Xu J, Liu X, Lu YQ. Cardioprotective Roles of Endothelial Progenitor Cell-Derived Exosomes. Frontiers in Cardiovascular Medicine. 2021; 8: 717536.

[33] Yan F, Liu X, Ding H, Zhang W. Paracrine mechanisms of endothelial progenitor cells in vascular repair. Acta Histochemica. 2022; 124: 151833.

[34] Kalluri R, LeBleu VS. The biology, function, and biomedical applications of exosomes. Science (New York, N.Y.). 2020; 367: eaau6977.

[35] Zha Y, Li Y, Lin T, Chen J, Zhang S, Wang J. Progenitor cell-derived exosomes endowed with VEGF plasmids enhance osteogenic induction and vascular remodeling in large segmental bone defects. Theranostics. 2021; 11: 397–409.

[36] Lee JH, Hah YS, Cho HY, Kim JH, Oh SH, Park BW, *et al*. Human umbilical cord blood-derived CD34-positive endothelial progenitor cells stimulate osteoblastic differentiation of cultured human periosteal-derived osteoblasts. Tissue Engineering. Part a. 2014; 20: 940–953.

[37] Katoh M. Therapeutics targeting angiogenesis: genetics and epigenetics, extracellular miRNAs and signaling networks (Review). International Journal of Molecular Medicine. 2013; 32: 763–767.

[38] Cui Y, Fu S, Sun D, Xing J, Hou T, Wu X. EPC-derived exosomes promote osteoclastogenesis through LncRNA-MALAT1. Journal of Cellular and Molecular Medicine. 2019; 23: 3843–3854.

[39] Jia Y, Zhu Y, Qiu S, Xu J, Chai Y. Exosomes secreted by endothelial progenitor cells accelerate bone regeneration during distraction osteogenesis by stimulating angiogenesis. Stem Cell Research & Therapy. 2019; 10: 12.

[40] Chen X, Hua W, Huang X, Chen Y, Zhang J, Li G. Regulatory Role of RNA N^6-Methyladenosine Modification in Bone Biology and Osteoporosis. Frontiers in Endocrinology. 2020; 10: 911.

[41] Yao Y, Bi Z, Wu R, Zhao Y, Liu Y, Liu Q, *et al*. METTL3 inhibits BMSC adipogenic differentiation by targeting the JAK1/STAT5/C/EBPβ pathway *via* an m^6A-YTHDF2-dependent manner. FASEB Journal: Official Publication of the Federation of American Societies for Experimental Biology. 2019; 33: 7529–7544.

[42] Wu Y, Xie L, Wang M, Xiong Q, Guo Y, Liang Y, *et al*. Mettl3-mediated m^6A RNA methylation regulates the fate of bone marrow mesenchymal stem cells and osteoporosis. Nature Communications. 2018; 9: 4772.

[43] Zhang Y, Gu X, Li D, Cai L, Xu Q. METTL3 Regulates Osteoblast Differentiation and Inflammatory Response via Smad Signaling and MAPK Signaling. International Journal of Molecular Sciences. 2019; 21: 199.

[44] Liu J, Yao Y, Huang J, Sun H, Pu Y, Tian M, *et al*. Comprehensive analysis of lncRNA-miRNA-mRNA networks during osteogenic differentiation of bone marrow mesenchymal stem cells. BMC Genomics. 2022; 23: 425.

[45] Sang Y, Kong P, Zhang S, Zhang L, Cao Y, Duan X, *et al*. SGK1 in Human Cancer: Emerging Roles and Mechanisms. Frontiers in Oncology. 2021; 10: 608722.